Influence of oxygen excitation by a RF plasma discharge on the flow field of atmospheric partially-premixed CH_4/O_2 and H_2/O_2 flames

K. Zähringer[*,1], K. Pliavaka[1], D. Thévenin[1]

[1] Lehrstuhl für Strömungsmechanik und Strömungstechnik (LSS),
Otto-von-Guericke-Universität Magdeburg, Germany

Abstract

This study investigates the changes induced by plasma-excited oxygen, in the flow field of partially-premixed CH_4 and H_2 flames under atmospheric conditions. Excited singlet oxygen is known to promote the chain mechanism reactions that control ignition and burning. Resulting modifications of the flame structure have been analyzed in previous works [1, 2] by different spectroscopic methods. The results of these measurements showed that the flow attaches closer to the burner surface and that the reaction zone becomes more concentrated toward the center of the system, when activating the plasma discharge. All these observations indicate strong changes in flow and flame topology induced by the plasma discharge. Therefore, additional velocity measurements have been carried out in this work, in order to verify these qualitative observations. The results of these measurements support the earlier presumption: when the plasma is on, the flow fields become more turbulent, higher velocities are observed and the flow turns preferentially toward the center of the burner.

Introduction

Excited singlet oxygen is known to promote the chain mechanism reactions that control ignition and burning, by excitation of internal degrees of freedom of the involved molecules. It has been demonstrated that pre-excitation of initial molecular reactants accelerates the formation of highly reactive radicals and lowers the self-ignition threshold, thereby intensifying combustion. The presence of excited (singlet) oxygen in H_2/O_2 and $CH_4/He/O_2$ mixtures leads to significant intensification of combustion processes [3-5].

The presence of excited oxygen in He/O_2 mixtures (up to 6% of O_2 in He) after leaving the plasma chamber has been detected by imaging and spectroscopy of $O_2(b_1 Sigma^+)$ at 762 nm for various discharge parameters and flow conditions. Resulting modifications of the flame structure have been analyzed in previous works [1, 2] by Raman scattering, spontaneous emission and laser-induced fluorescence (LIF) of the OH radical and, for CH_4, by the spontaneous emission of CH and C_2.

The results of these measurements indicated noticeable modifications of the underlying flow topology. It could be observed that the flow attaches closer to the burner surface and that the reaction zone becomes more concentrated toward the center of the system when activating the plasma discharge. Additionally, the burning regime was modified, with additional nitrogen sucked in from the surrounding air toward the burning region. All these observations proved strong changes in flow and flame topology induced by the plasma discharge.

Therefore, additional velocity measurements have been carried out in the current project to verify these qualitative observations. The results of these measurements support the earlier presumption: when the plasma is on, a higher turbulence level if found in the flow fields, higher velocities are observed and the flow turns toward the center of the burner. This explains as well, why more nitrogen from the surrounding air can be transported into the center of the flame under such conditions.

Experimental set-up

A detailed description of the actual experimental set-up of our plasma-burner system is given in [1]. Here, only the main features are summarized. A High-Voltage Radio-Frequency (HVRF) generator coupled with a discharge chamber (photograph on Fig.1) is used for the production of excited oxygen. It relies on a so-called warm discharge, which is often used for fuel conversion [6, 7]. Electron energy values of such discharges are in the range of 1–3 eV, suitable for singlet oxygen production, as demonstrated in previous studies of our group. The generator delivers pulses up to 25 kV at a frequency of 1 MHz, with output power up to 450 W.
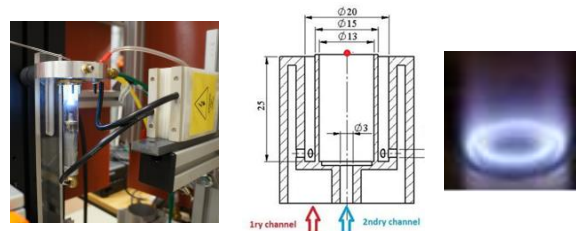

Fig. 1: Experimental set-up, with photograph of the plasma generator (left), burner sketch (center) and resulting flame (right)

This discharge chamber is integrated within a concentric burner in a partially-premixed flame configuration (Fig. 1). It consists of two inlet channels: the outer

primary for the fuel-oxidizer mixture and, in the center, the secondary injection for the excited-oxygen/He mixture. Only the gas mixture of the secondary injection flows through the plasma chamber. The fuels considered during the present study are methane and hydrogen.

The secondary flow is constituted by 3.2% (in volume) of oxygen diluted in helium, since this ratio has been found to ensure the highest production rate of excited oxygen in the system [1]. All other gases are introduced through the surrounding primary channel. In the case of the methane flame the total flow rates for all gases range from 1.2 to 1.6 m^3/h, resulting in outlet velocities of 1.76-2.65 m/s in the primary and 0.65 m/s in the secondary channel and thermal powers up to 2.87 kW for equivalence ratios from 0.54 to 1. For hydrogen flames the equivalence ratios and flow rates through the secondary channel have been kept the same. Then, the flow rate through the primary channel must be adapted, leading to velocities of 1.4-2.2 m/s. The flame thus delivers a thermal power of up to 0.8 kW.

Electrical power measurements for the plasma and detection of excited oxygen in the afterglow of the discharge, via observation of the $O_2(b^1\Sigma^+)$ transition at 762 nm, are done as described in [2]. These measurements proved the existence of excited oxygen at the height of the burner outlet (Fig. 2a.) and served for the regulation of the plasma power (Fig. 2b.).

Several parameters, in particular stoichiometry and plasma power have been systematically evaluated during our measurements. Instantaneous snapshot and mean velocity fields have been acquired by particle-image velocimetry (PIV) in the flame and in the corresponding non-ignited mixtures. A LaVision ImagerIntense camera has been used for the PIV measurements in the center plane of the burner. A NewWave Nd:YAG laser served for illumination of the Aerosil200 SiO_2 seeding particles. Note that those seeding particles could only be introduced into the primary flow. A home-made fluidized bed seeder has been used for this purpose. For a proper function of the plasma chamber, the secondary, excited

oxygen flow, traversing the plasma chamber, should not contain any particles. This procedure could obviously lead to seeding inhomogeneities. Due to strong mixing processes within the burner, it is expected that measurements at the burner outlet are possible with a suitable, homogeneous seeding.
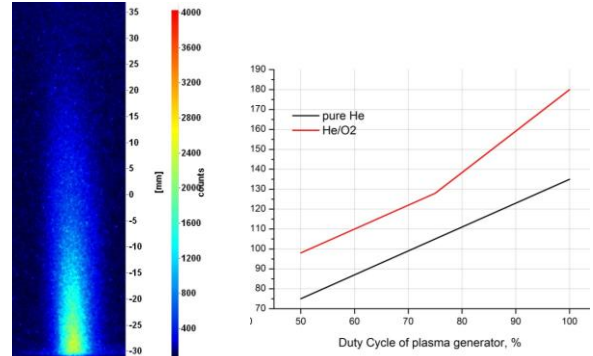
a. Excited oxygen jet at the outlet of the plasma chamber, with 3.2% O_2 in He (98 W)

b. Discharge power (in Watt) measured in function of the duty cycle of the plasma generator for pure He and 3.2% O_2 in He

Fig. 2: excited oxygen and plasma power

Since the overall seeding density is rather low, a combined PIV-PTV algorithm (Davis 8.1) has been used for evaluation. After scaling, background subtraction and masking of reflecting burner surfaces a multipass PIV-calculation was done with 128^2 to 64^2 pixel interrogation areas and 50% overlap. Then a PTV evaluation step is added with a 12-pixel correlation window. The individual snapshot results are then transferred to a grid and postprocessed to eliminate spurious vectors. Finally the mean velocity fields, shown in what follows, have been calculated from the 50 instantaneous velocity results.
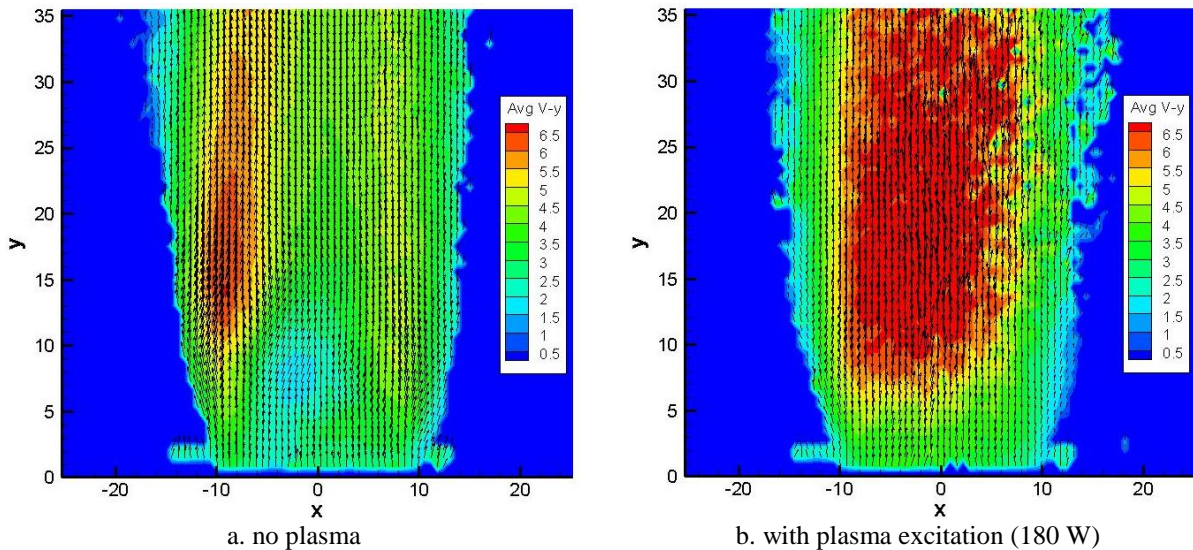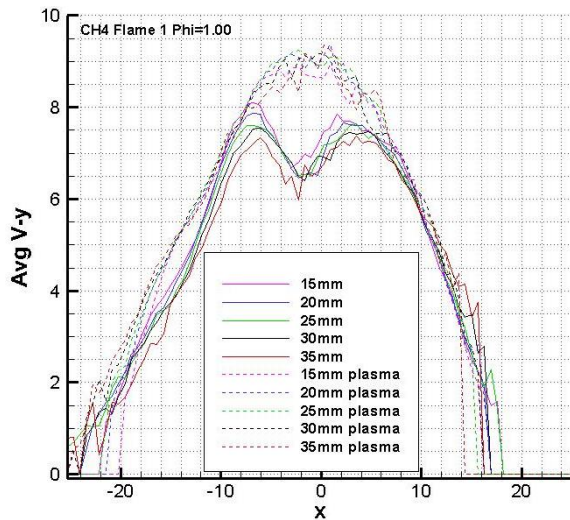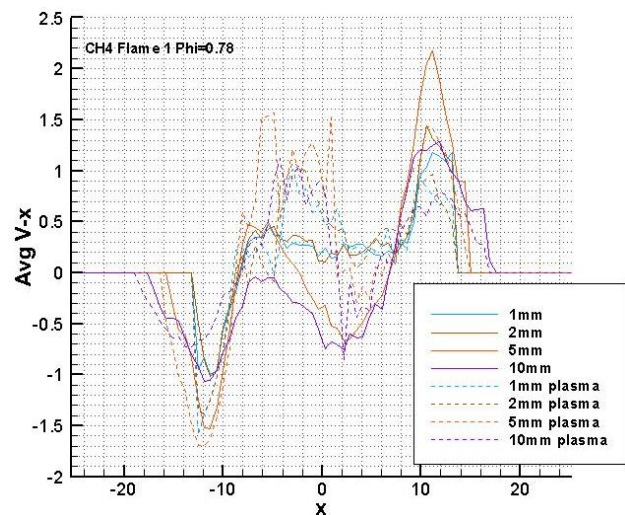

a. no plasma

b. with plasma excitation (180 W)

Fig. 3: mean velocities (m/s) in a H_2-flame (Φ=1.0): vectors and vertical velocity component (colored)

Results

A first impression of the difference between the velocity field in the flame without and with plasma excitation is given in figure 3. The mean velocity vectors and vertical velocity components v_y are shown there for a hydrogen flame with an equivalence ratio $\Phi=1$. The same color scale is used for both figures. Figure 3a. represents the results for the non-excited case. The velocity field is, due to asymmetries within the burner geometry, not completely axisymmetric. It shows in this cut two concentric zones of higher velocity at a radius of about 10mm. When adding excited oxygen (Fig. 3b.), the flow topology changes completely, and a high-velocity region is observed in the whole central region of the flame. In this region, vertical velocities of about 6.5 m/s are measured. It can also be recognized on these images, that larger fluctuations appear in the high-speed region. Within the high-speed, central region, the mean image of the case with plasma (Fig. 3b) shows noticeable changes in velocity direction and magnitude at small scale. This is even more obvious when looking at instantaneous snap-shots, which show much larger variations in the case with plasma.

The higher velocities in the flame with plasma can be directly explained by the higher temperature of the plasma flow and by the jet-like outlet of the plasma-chamber, where the secondary flow is accelerated rather strongly during excitation.

The observed modifications of the velocity fields are similar in hydrogen and methane flames. Especially in the upper part of the flame, the velocity profiles change a lot. This is represented in figure 4a. for the vertical velocity component v_y of a methane flame ($\Phi=1$). The M-like velocity distribution changes to a triangular-shaped distribution with higher peak velocities.

Due to the plasma, also the radial velocity v_x component changes a lot. This is found to be particularly strong in the lower part of the flame (Fig. 4b.). Locally the magnitude $|v_x|$ increases noticeably when the plasma is on. Additionally local inversions of the flow direction can be recognized. This can explain the increasing entrainment of surrounding air with its nitrogen content, as observed during Raman measurements in the same system [1].

a. vertical component v_y, $\Phi=1.0$, 15-35 mm after the burner outlet

b. horizontal component v_x, $\Phi=0.78$, 1-10mm after the burner outlet

Fig. 4: mean velocities (m/s) in the CH_4-flame with and without plasma (plasma power 180 W)

The previously mentioned Raman measurements revealed the onset of reaction in unburned methane gas mixtures due to the presence of excited oxygen (Fig. 5a.), while this effect could not be observed in hydrogen mixtures (Fig. 5b.). Since these measurements had only been done on a straight line 1 mm over the outlet of the burner, a possible explanation of this phenomenon was a changed flow pattern. Therefore, velocities have also been measured in the unburned mixtures for both fuels.

These additional PIV measurements reveal similar modifications of the velocity profiles. Hence, the modifications in flow topology induced by the plasma discharge appear to be quite the same under reacting and non-reacting conditions. Higher radial velocities v_x are

systematically observed, showing again local inversions of flow direction for some conditions (Fig. 6a. and 7a.). The vertical component v_y (Fig. 6b. and 7b.) shows a higher peak and a large high-velocity region near the axis of the system.

In the case of methane (Fig. 6b.) the measured axial profiles do not change considerably in this non-reacting flow when activating the plasma discharge. The situation is different for the case of hydrogen (Fig. 7b.). Here, the initial M-like structure of the axial velocity profile observed without plasma case changes to a triangular shape when activating the plasma discharge in this non-reacting flow. This is similar to the observation discussed

in connection with figure 4a for the burning methane flame.

It appears that modifications in flow topology are not responsible for the onset of reaction observed in the non-reacting methane flow when activating the discharge. Therefore, this observation should be a result of pure kinetics. The presence of excited oxygen and the slight increase in temperature, both induced by plasma activation, appear to be responsible for the onset of reaction in the methane flow, while they are not sufficient to initiate reaction in the hydrogen flow.
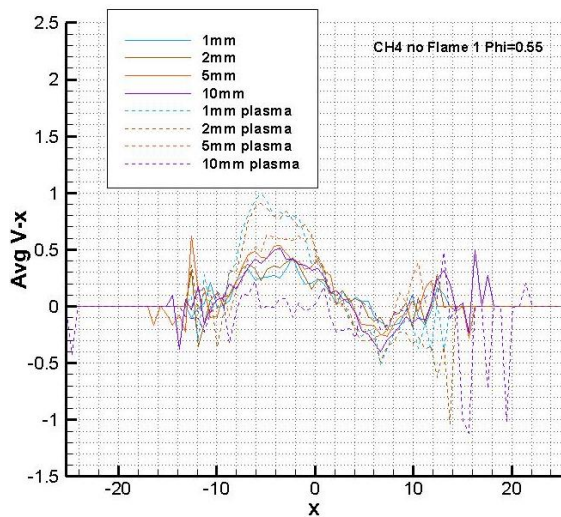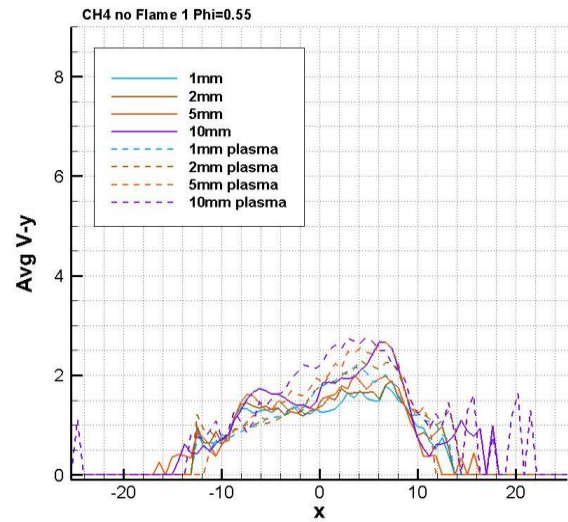
a. CH$_4$ b. H$_2$
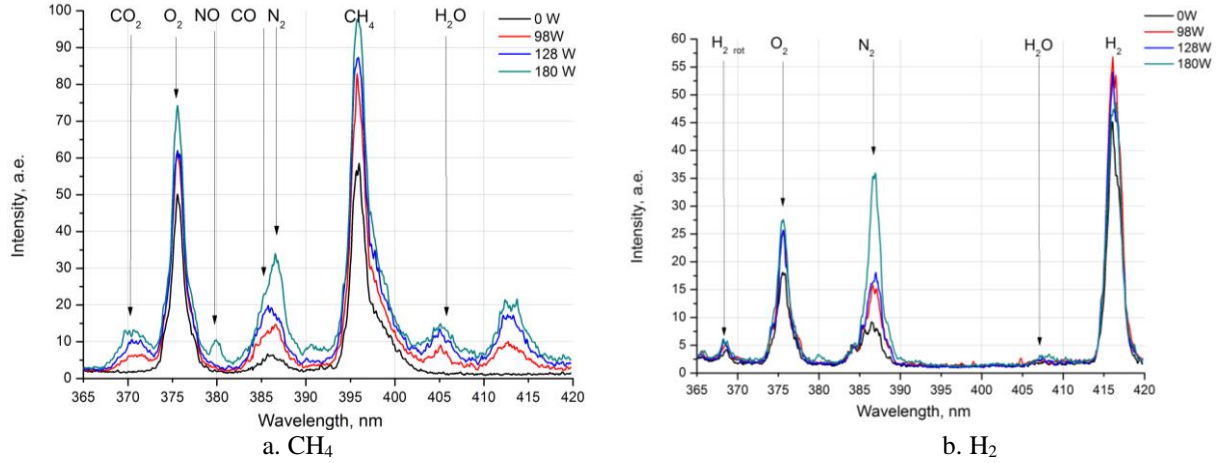
Fig. 5: Mean Raman spectra of the non-ignited mixtures (ϕ=0.55) for different power inputs

a. horizontal component v$_x$, Φ=1.0,   b. vertical component v$_y$, Φ=1.0,
1-10 mm after the burner outlet   1-10mm after the burner outlet

Fig. 6: Mean velocities (m/s) in the unburnt CH$_4$-mixtures with and without plasma (plasma power 180 W)
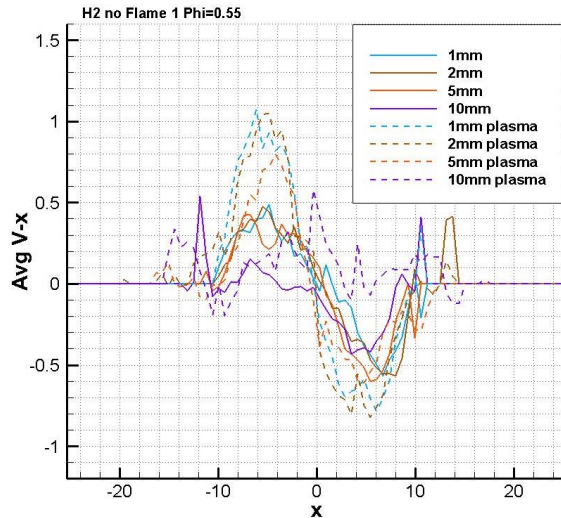
a. horizontal component v_x, Φ=0.55,
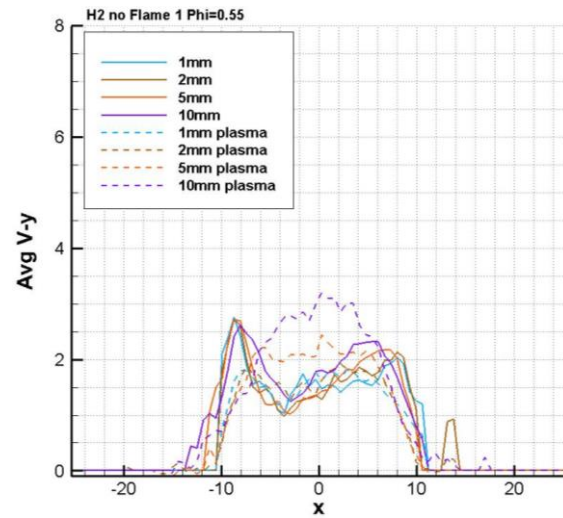1-10 mm after the burner outlet

b. vertical component v_y, Φ=0.55,
1-10mm after the burner outlet

Fig. 7: Mean velocities (m/s) in the unburnt H_2-mixtures with and without plasma (plasma power 180 W)

Conclusions

This study presents results of velocity measurements for plasma-excited combustion. Excited oxygen is produced under atmospheric conditions using a warm plasma discharge. The plasma discharge has been integrated into a burner leading to a partially-premixed flame configuration. Resulting modifications of the velocity fields when activating the plasma discharge have been analyzed by a combined PIV-PTV algorithm. It has been observed that higher velocity fluctuations are present under plasma excitation. Higher velocities are found in a much larger region around the axis, when the plasma is on. In some cases the radial velocity component changes its direction when switching the plasma on, thus leading locally to a reversed flow. This phenomenon could explain the additional entrainment of surrounding air (and thus nitrogen) into the flame, which had been observed before by Raman measurements. Similar changes in the velocity fields are observed both for hydrogen mixtures and methane mixtures. Therefore, the observed differences concerning the onset of reaction in the cold mixtures, found only for methane and not for nitrogen, must be a direct result of plasma activation: the presence of excited oxygen in addition with a slight increase in temperature is hence probably responsible for the initiation of reactions in the methane case.

Acknowledgements

References

1. K. Zähringer; K. Pliavaka; D. Thévenin; U. Riedel, in: *45th AIAA Plasmadynamics and Lasers Conference, AIAA Aviation and Aeronautics Forum and Exposition*, Atlanta (USA), 2014; Vol. PDL-04, pp 2014-42241.
2. K. Pliavaka; F. Pliavaka; S. Gorbatov; D. Thévenin; K. Zähringer, in: *European Combustion Meeting*, Lund, Sweden, 2013; pp P1-88.
3. A. Bourig; D. Thévenin; J.-P. Martin; G. Janiga; K. Zähringer, Proceedings of the Combustion Institute 32 (2009) 3171-3179.
4. V. V. Smirnov; O. M. Stelmakh; V. I. Fabelinsky; D. N. Kozlov; A. M. Starik; N. S. Titova, Journal of Physics D: Applied Physics 41 (2008) 192001 (6p).
5. K. Zähringer; A. Bourig; D. Thévenin, in: *6th International Workshop and Exhibition on Plasma Assisted Combustion*, Heilbronn, Germany, 2010; pp 45-47.
6. A. Gutsol; A. Rabinovich; A. Fridman, Journal of Physics D: Applied Physics 44 (27) (2011) 274001
7. A. Fridman, Plasma Chemistry, Cambridge University Press, New York, 2008.